the soma. The conductance time course was proportional to te^{-t}, with a peak of 120 nS. These properties allowed a single presynaptic action potential to evoke an action potential in an inhibitory neuron. Fast IPSPs developed on the soma and adjacent compartments, with conductance time course rising linearly over 2 ms and then decaying with a time constant of 7 ms; the peak value was different in different simulations. The peak value was usually 10 nS, but values from 0 to 15 nS have been investigated. Slow IPSPs developed in the dendrites; they grew steadily over 40 ms and decayed with a time constant of 100 ms. The time course of the simulated slow IPSP after a local shock is shown in (*14*, figure 1). The output of pyramidal neurons was distributed to follower cells after a delay proportional to cell separation along the long axis of the array; this delay corresponded to axon conduction delays. An axon conduction velocity of 0.5 m/s was used. Details are in (*14*). Programs were written in Fortran, optimized for the IBM 3090 vector compiler. A simulation of 3 s of neural activity consumed about 6.6 hours of computation time on the 3090 computer.

31. There is little precise experimental guidance on how to do this. The necessary experiment would involve synaptically isolating all the neurons in a population from each other without changing any of their intrinsic properties and then characterizing the spontaneous activities of a large sample of the cells.
32. There is another type of synchronized activity that occurs in hippocampal slices wherein all forms of chemical synaptic actions have been blocked. This activity consists of repeating, large-amplitude population spikes [C. P. Taylor and F. E. Dudek, *Science* **218**, 810 (1982); J. G. R. Jefferys and H. L. Haas, *Nature* **300**, 448 (1982)], probably synchronized by electric field interactions [C. P. Taylor and F. E. Dudek, *J. Neurophysiol.* **52**, 126 (1984); R. D. Traub, F. E. Dudek, C. P. Taylor, W. D. Knowles, *Neuroscience* **14**, 1033 (1985)]. We shall not treat this type of activity in this article because during partially synchronized bursts of the type we are considering, the extracellular potentials in the cell body layer are too small to be detected with present recording methods.
33. S. J. Korn *et al.*, *J. Neurophysiol.* **57**, 325 (1987).
34. P. Dutar and R. A. Nicoll, *Nature* **332**, 156 (1988).
35. O. S. Vinogradova, E. S. Brazhnik, A. M. Karanov, S. D. Zhadina, *Brain Res.* **187**, 353 (1980).
36. J. Konopacki, M. B. MacIver, B. H. Bland, S. H. Roth, *ibid.* **405**, 196 (1987). It has been suggested, however, that carbachol may simply alter the intrinsic properties of hippocampal neurons [L.-W. S. Leung and C. Y. Yim, *Neurosci. Res. Commun.* **2**, 159 (1988)].
37. R. Malisch and T. Ott, *Neurosci. Lett.* **28**, 113 (1982).
38. A. P. Rudell, S. E. Fox, J. B. Ranck, *Exp. Neurol.* **68**, 87 (1980).
39. G. Buzsáki, E. Grastyán, J. Czopf, L. Kellényi, O. Prohaska, *Brain Res.* **225**, 234 (1981).
40. L.-W. S. Leung, *J. Neurophysiol.* **52**, 1051 (1984).
41. R. D. Traub, R. Miles, R. K. S. Wong, *IEEE Eng. Med. Biol. Mag.* **7**, 31 (1988).
42. G. Buzsáki, E. Grastyán, I. N. Tveritskaya, J. Czopf, *Electroenceph. Clin. Neurophysiol.* **47**, 67 (1979).
43. G. Buzsáki and F. H. Gage, in *Memory Mechanisms: A Tribute to G. V. Goddard*, M. Corballis, K. White, W. Abraham, Eds. (Erlbaum, Hillsdale, NJ, in press).
44. G. Buzsáki, *Brain Res.* **398**, 242 (1986); S. S. Suzuki and G. K. Smith, *Electroenceph. Clin. Neurophysiol.* **67**, 348 (1987).
45. Supported by IBM, The Klingenstein Foundation, and NIH. We thank G. Buzsáki and L. S. Schulman for helpful discussions and A. Rossi for invaluable assistance in optimizing Fortran code.

Research Articles

Hydrogen Tunneling in Enzyme Reactions

YUAN CHA,* CHRISTOPHER J. MURRAY,† JUDITH P. KLINMAN‡

Primary and secondary protium-to-tritium (H/T) and deuterium-to-tritium (D/T) kinetic isotope effects for the catalytic oxidation of benzyl alcohol to benzaldehyde by yeast alcohol dehydrogenase (YADH) at 25 degrees Celsius have been determined. Previous studies showed that this reaction is nearly or fully rate limited by the hydrogen-transfer step. Semiclassical mass considerations that do not include tunneling effects would predict that $k_H/k_T = (k_D/k_T)^{3.26}$, where k_H, k_D, and k_T are the rate constants for the reaction of protium, deuterium, and tritium derivatives, respectively. Significant deviations from this relation have now been observed for both primary and especially secondary effects, such that experimental H/T ratios are much greater than those calculated from the above expression. These deviations also hold in the temperature range from 0 to 40 degrees Celsius. Such deviations were previously predicted to result from a reaction coordinate containing a significant contribution from hydrogen tunneling.

ELECTRON TUNNELING IN PROTEINS HAS BEEN EXTENSIVELY studied (*1*). Rapid, long-distance electron transfer between donor and acceptor sites appears well established (*2*). Although quantum-mechanical tunneling of particles heavier than the electron has been actively studied in solid-state, gas-phase, and solution reactions (*3*), nuclear tunneling in proteins has received relatively little attention. In this article we present evidence that nuclear tunneling contributes to enzymatic reaction rates under biologically relevant conditions. The phenomenon of hydrogen tunneling is an especially promising area to pursue, in that hydrogen has a small mass and the kinetics of protium can be compared with its isotopes, deuterium and tritium (*4*). Detection of H-tunneling in chemical reactions has relied heavily on either the detection of anomalously large isotope effects or the comparison of Arrhenius plots for H transfer to that for either D or T. Given the enhanced probability for H tunneling, greater curvature is anticipated in its Arrhenius plot. A manifestation of this property is a decrease in the magnitude of the intercept obtained on extrapolation to infinite temperature such that the Arrhenius prefactors are ordered as $A_H < A_D < A_T$ (*3*).

The detection of nuclear tunneling in enzymatic reactions presents several experimental challenges. In enzymatic systems, diffusional binding processes, rather than chemical transformations, may limit catalysis (*5, 6*). Even in the event that an elementary chemical step can be isolated at a single temperature, alterations in temperature can lead to changes in rate limitation, giving rise to artifactual curvature in Arrhenius plots. In 1985 Saunders (*7*) demonstrated that the relation of D/T to H/T kinetic isotope effects can show significant deviations from semiclassical limits when tunneling contributes to the H-transfer step. We have experimentally verified

The authors are at the Department of Chemistry, University of California, Berkeley, CA 94720. The order of the first two authors is arbitrary.

*Present address: Department of Chemistry, Rockefeller University, New York, NY 10021.
†Present address: Department of Chemistry and Biochemistry, University of Arkansas, Fayetteville, AR 72701.
‡To whom correspondence should be sent.

Table 1. De Broglie wavelengths; $\lambda = h/(2mE)^{1/2}$, where m is the mass of the particle and E = 20 kJ/mol.

Property	Particle				
	e^-	H	D	T	C
Mass (amu)	1/1750	1	2	3	12
λ (Å)	27	0.63	0.45	0.36	0.18

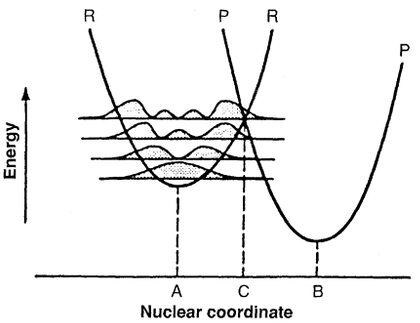

Fig. 1. Reaction-coordinate diagram for the conversion of reactant A on the R potential surface to product B on the P potential surface. Thermal activation leads to an over-the-barrier process at transition state C. Vibrational states have been shown for the reactant A. The superposition of wave functions for each vibrational level illustrates the increasing barrier penetration with increasing temperature.

this prediction in an enzymatic reaction. This method does not require knowledge of intrinsic isotope effects nor complete rate limitation by chemistry. The consequences of the detection and evaluation of nuclear tunneling in enzyme reactions include the description of reaction barrier shapes and an evaluation of the role of protein dynamics in enzyme catalysis.

Basic theory. The phenomenon of tunneling results from the wave-particle duality of matter and increases in probability with increasing de Broglie wavelength λ. The de Broglie wavelengths for a range of particles with a total energy of 20 kJ/mol are shown in Table 1. The large wavelength of the electron (27 Å) leads to a very high uncertainty in its position and a high tunneling probability. With regard to protium, a calculated wavelength of ~1 Å is near the length of a reaction coordinate, which also predicts a significant departure from classical behavior. The mass of D and T relative to H decreases their wavelengths and tunneling probabilities, respectively.

The factors that contribute to hydrogen tunneling can be examined more closely with a reaction coordinate diagram (Fig. 1). The nontunneling contribution to the conversion of reactant A to product B occurs by an over-the-barrier process, at the transition state, C. This process occurs from a series of molecular vibrational levels that are shown superimposed on the electronic potential energy surface for the reactant. Within each vibrational level a wave function has been drawn to illustrate the increasing overlap of the reactant wave function with the product state as the temperature is elevated and excited vibrational states are occupied. At room temperature, the molecule is almost exclusively in the zero-point vibrational level. The factors that lead to an increased tunneling probability from this state are a small particle mass (increased wavelength λ) and a narrow barrier width (greater overlap of the wave function for A into B).

Mathematical treatments of tunneling vary depending on the choice of a barrier shape. A commonly used barrier is the truncated parabola, which leads to the simplified tunneling correction of Eq. 1 (*3*)

$$Q_t(L) = \frac{h\nu\ddagger}{2kT \sin(h\nu\ddagger/2kT)} \quad (1)$$

where h is Planck's constant, k is Boltzmann's constant, $\nu\ddagger$ is the reaction-coordinate frequency, T is the experimental temperature, and L = H, D, or T. The magnitude of $\nu\ddagger$, which is related to barrier curvature, can be formulated in the context of Hooke's law for a vibrating bond

$$\nu\ddagger = (1/2\pi)(F/m_L)^{1/2} \quad (2)$$

where m_L is the reduced mass of the transferred particle (*8*) and F is the force constant of the vibrating bond (*9*). From Eq. 2, the key features that determine the tunneling correction at room temperature are the mass of the particle undergoing transfer and the reaction-coordinate shape. For reaction coordinates characterized by large values for F (for example, high, narrow barrier shapes), $\nu\ddagger$ is large and tunneling corrections are important, whereas small values of F (for example, short, flat barrier shapes) lead to low values for $\nu\ddagger$ and little or no tunneling.

These properties can be found in simple hydrogen-transfer reactions on enzyme surfaces. Enzymes function by reducing reaction barrier heights, which for a fixed transfer distance may be expected to decrease both F and the frequency of tunneling. However, there are three features that may appreciably enhance tunneling at enzyme active sites. The first concerns the magnitude of internal equilibrium constants for the interconversion of substrates and products at enzyme active sites. A number of enzymatic reactions have been shown to have internal equilibrium constants, K_{eq}, that are altered relative to the value of K_{eq} in solution, with the value of K_{eq} (internal) tending toward unity (*10*). The probability of hydrogen tunneling increases as the energy of reactants and products approach one another (*11, 12*).

A second feature concerns the role of solvation in catalysis. For solution reactions, reorganization of solvent must accompany elementary bond-making and bond-breaking processes in order to satisfy changes in charge distribution, hydrogen-bonding requirements, and so forth. This coupling of solvent motion to hydrogen transfer may increase the mass of the transferred particle and reduce the probability for tunneling (*13*). On an enzyme surface, however, substrate binding leads to displacement of bound water (*14*), such that the critical role of solvation is assumed by protein side chains. Since transition-state theory predicts that protein side chains will be positioned to stabilize optimally transition state (rather than ground state) structure (*15*), little or no structural reorganization may be required in the bond cleavage step.

Barrier width may also facilitate tunneling in enzyme catalysis. Secondary isotope effects in the catechol *O*-methyltransferase reaction suggest that the transition state for enzymic methyl transfer has a decreased bond order relative to the model reaction (*16*). Such "close packing" may occur between a substrate and a catalytic side chain, as well as between two substrates in the transition state. To the extent that reduced barrier widths can be achieved on enzyme surfaces, tunneling may arise with a greater frequency than in bulk solvent.

Isotope effects as probes. Many studies of isotope effects have focused on a comparison of two rate-constant ratios, k_H/k_D and k_H/k_T. In the absence of tunneling, k_H/k_D and k_H/k_T are related by reduced-mass considerations (*17*)

$$(k_H/k_D)^{1.44} = k_H/k_T \quad (3)$$

The validity of Eq. 3 rests largely on the assumption that the semiclassical isotope effect is dominated by differences in C–L (L = H, D, or T) stretching frequencies, which can be treated as harmonic oscillators. A number of investigators have examined the consequences of hydrogen tunneling to Eq. 3, and have found little deviation from an exponent of 1.44 (*3*). This observation can be understood qualitatively in the context of a reaction where protium, but neither a deuterium nor a tritium atom, tunnels. Since protium

is the common isotope relating the left- and right-hand sides of Eq. 3, tunneling results in a relatively small perturbation of the semiclassical relation between D and T effects.

Saunders, using model vibrational analysis calculations (*7*), has demonstrated a subtle but important deviation from Eq. 3. The semiclassical relation between the two isotope effects, k_H/k_T and k_D/k_T, can be formulated in terms of reduced-mass considerations, leading to Eq. 4

$$(k_D/k_T)^{3.26} = k_H/k_T \quad (4)$$

The key difference between Eqs. 3 and 4 is that in Eq. 4 tritium, not protium, is the common atom. Under conditions such that H tunnels with a greater probability than either D or T, an inflated value for the experimentally measured value of k_H/k_T results. Comparison of $(k_H/k_T)_{obs}$ to a value calculated from the experimentally measured k_D/k_T (with the use of Eq. 4) leads to the following inequality:

$$(k_D/k_T)^{3.26} = (k_H/k_T)_{calc} < (k_H/k_T)_{obs} \quad (5)$$

Thus Eq. 5 provides a simple and direct test of hydrogen tunneling.

A major consideration in the application of Eq. 5 to enzyme reactions is the ability to isolate a single chemical step. In particular, it is important to question whether the inequality in Eq. 5 can arise artifactually through the introduction of multiple rate-limiting steps. Many workers (*18–20*) have pointed out that the presence of non-isotopically sensitive rate-limiting steps can cause Eqs. 3 and 4 to be invalid. This point can be addressed through the formulation of H/T and D/T isotope effects as introduced by Northrop (*19*):

$$(V/K_m)_H/(V/K_m)_T = \frac{k_H/k_T + C_H}{1 + C_H} \quad (6)$$

$$(V/K_m)_D/(V/K_m)_T = \frac{k_D/k_T + C_D}{1 + C_D} \quad (7)$$

where V represents the maximal velocity, K_m is the Michaelis constant, and C is the commitment to catalysis. As shown, observed V/K_m isotope effects may be reduced from intrinsic isotope effects by C. Analogous equations have been written for H/D and H/T isotope effects (*19*). An important difference exists, however, between previously published formulations and the expressions in Eqs. 6 and 7. As discussed by Northrop, equations for H/T and H/D isotope effects contain the common parameter, C_H. Thus the expressions for H/T and H/D can be combined, so that a solution for the intrinsic isotope effect can be expressed in terms of experimentally measured H/T and H/D effects (*19*).

Inspection of Eqs. 6 and 7, however, indicates different commitments, since in Eq. 6 the frame of reference is C–H bond cleavage, whereas in Eq. 7 it is C–D bond cleavage. This key feature leads to reduction of the commitment term in Eq. 7 relative to Eq. 6 by the magnitude of the intrinsic H/D isotope effect. Thus, to the extent that steps other than C–L bonding limit enzyme turnover, the experimentally measured H/T isotope effect is reduced relative to the intrinsic H/T effect by a significantly greater extent than is the D/T isotope effect. This effect results in a suppression of the magnitude of the observed H/T isotope effect relative to D/T, leading to the inequality (*21*)

$$(k_D/k_T)^{3.26} = (k_H/k_T)_{calc} > (k_H/k_T)_{obs} \quad (8)$$

We note that Eqs. 5 and 8 predict opposite relations of D/T and H/T isotope effects under conditions of kinetic complexity (Eq. 8) versus hydrogen tunneling (Eq. 5). Thus we conclude that conditions such that Eq. 5 holds provide unambiguous evidence for hydrogen tunneling in enzyme reactions.

Experimental comparison of k_D/k_T to k_H/k_T. The yeast alcohol dehydrogenase (YADH) reaction was chosen as a test reaction for several reasons. First, previous studies of primary isotope effects have implicated a rate-limiting hydride transfer step and an internal equilibrium constant near unity for the oxidation of benzyl alcohol by nicotinamide adenine dinucleotide (NAD^+) (*22*)

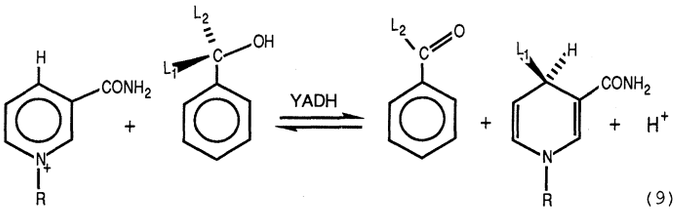

Second, early studies of secondary isotope effects in both the yeast and horse liver ADH reactions had indicated anomalously large values that were incompatible with other probes of transition-state structure (*23, 24*). Such anomalies have been interpreted in terms of coupled motion between the primary (L_1) and secondary (L_2) hydrogens at the methylene carbon of substrate undergoing oxidation (*24, 25*), such that motion at the noncleaved position (L_2) becomes part of the reaction coordinate (Fig. 2). In this case, it becomes difficult to distinguish clearly between primary and secondary isotope effects, as the secondary effect becomes inflated and the primary effect reduced (*24, 25*). In subsequent efforts, force-field calculations based on semiclassical mechanics could not fit the experimental data. Thus Huskey and Schowen proposed a quantum-mechanical correction and found that the experimental data for ADH could be satisfied by incorporation of a tunneling correction of $Q_t(H)/Q_t(D) = 1.19$ for the secondary isotope effect and $Q_t(H)/Q_t(D) = 1.57$ for the primary effect (*26*).

Our experimental protocol involved the enzymatic conversion (Eq. 9) of a mixture of tritiated benzyl alcohol [randomly tritiated in the (*S*)- and (*R*)-positions at C-1] and [^{14}C]benzyl alcohol (ring-labeled) to benzaldehyde and reduced NAD^+ (NADL). Identical conditions apply to both D/T and H/T isotope effect measurements (*27*). In all cases, product aldehyde was converted to semicarbazone with semicarbazide to prevent reversal of Eq. 9 as well as non-enzymatic oxidation of aldehyde to acid. Product semicarbazones were separated from alcohol and cofactor by reversed-phase high-

Table 2. Primary kinetic isotope effects (V/K_m isotope effects) for oxidation of benzyl alcohol to benzaldehyde at 25°C, *p*H 8.5. Conditions for determining isotope effects were 80 m*M* glycine (*p*H 9.3), 10 m*M* semicarbazide (*p*H 5.6), 10 m*M* NAD^+ [K_m = 5 m*M* (*39*)], 2 m*M* benyzl alcohol [K_m = 22 m*M* (*39*)], and 800 U/ml YADH (Boehringer Mannheim Biochemicals). Errors are standard deviations based on five or more determinations at 25°C. The term (k_H/k_T)calc was calculated from $[(k_D/k_T)obs]^{3.26}$. Errors were calculated from $\partial H/T = 3.26\ [(k_D/k_T)obs]^{2.26}\ \partial D/T$.

(k_D/k_T)obs	(k_H/k_T)calc	(k_H/k_T)obs
1.72 ± 0.03	5.86 ± 0.33	7.15 ± 0.17
1.70 ± 0.03	5.64 ± 0.32	7.00 ± 0.07
1.76 ± 0.03	6.31 ± 0.35	7.23 ± 0.10
1.72 ± 0.05	5.86 ± 0.56	
1.73 ± 0.02*	5.91 ± 0.20*	7.13 ± 0.07*

*Average values with standard deviations.

Fig. 2. Transition-state geometry for the transfer of the primary hydrogen (L_1) between carbon centers C_1 and C_2. As illustrated, the motion of the secondary hydrogen (L_2) is coupled to that of the transferred atom (L_1). [Adapted from (*26*) with permission © American Chemical Society.]

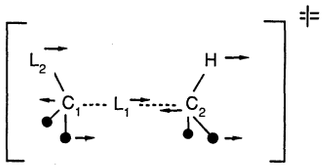

Table 3. Secondary kinetic isotope effects (V/K_m isotope effects) for oxidation of benzyl alcohol to benzaldehyde at 25°C, *p*H 8.5. Experimental conditions were as described in Table 2.

(k_D/k_T)obs	(k_H/k_T)calc	(k_H/k_T)obs
1.03 ± 0.01	1.10 ± 0.03	1.37 ± 0.02
1.03 ± 0.01	1.10 ± 0.03	1.33 ± 0.01
1.03 ± 0.004	1.10 ± 0.01	1.35 ± 0.04
1.04 ± 0.02	1.14 ± 0.07	
1.03 ± 0.006*	1.11 ± 0.02*	1.35 ± 0.015*

*Average values with standard deviations.

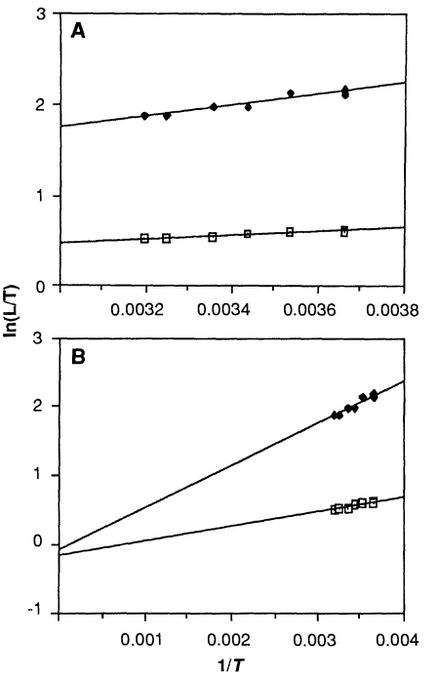

Fig. 3. Arrhenius plots for primary k_H/k_T (◆—◆) and k_D/k_T (□—□) isotope effects. (**A**) The data are shown in the experimental temperature range, 0° to 40°C. (**B**) A full plot, showing the extrapolation of experimental data to infinite temperature. These data indicate a difference in activation energy for C–H versus C–D bond cleavage of $E_D - E_H$ = 3/3 kJ/mol and A_H/A_D = 1.1 ± 0.1, obtained from $E_D - E_H = (E_D - E_T) - (E_H - E_T)$ and $A_H/A_D = (A_H/A_T)/(A_D/A_T)$.

performance liquid chromatography and the ratio of ^3H to ^{14}C was determined by scintillation counting. Ratios of ^3H to ^{14}C in product semicarbazones at early and late times yielded the secondary isotope effect, whereas comparison of ^3H in NADL to ^{14}C in semicarbazones yielded the primary isotope effect (*28*).

The results of primary isotope effect measurements at 25°C are summarized in Table 2. Within each experiment, at least five time points at different conversions were determined, leading to an average error of 2 percent for both k_D/k_T and k_H/k_T values. Comparison of multiple experiments also indicates very small error, with a reproducibility of 1 percent for k_D/k_T and k_H/k_T. Calculated values for k_H/k_T were obtained from experimental k_D/k_T values with Eq. 4. In all instances the calculated value for k_H/k_T was significantly less than the observed k_H/k_T, with the data in Table 2 requiring an exponent of 3.58 ± 0.09 for agreement between the measured k_D/k_T and k_H/k_T values. Although 3.58 may not appear different from 3.26, the theoretical upper limit for the exponent in Eq. 4 is 3.34 (*29*). Thus the data in Table 2 provide clear evidence for a tunneling component in the transfer of hydrogen between substrate and cofactor. It is important to point out that comparison of D/T and H/T isotope effects requires the determination of high-precision D/T and H/T isotope effects, since D/T errors propagate into the calculated value for H/T.

A particularly compelling example of the breakdown of Eq. 4 comes from a comparison of secondary isotope effects. As discussed above and illustrated in Fig. 2, there is evidence for coupling of the motion between the primary and secondary hydrogens at C-1 of alcohol in the course of enzyme-catalyzed oxidation (*24, 25*). One would then expect the contribution of tunneling to the transfer of L_1 to be propagated into the noncleaved position (L_2). Model calculations have demonstrated the extent of the breakdown of Eq. 4 for secondary isotope effects as a function of the degree of coupled motion between L_1 and L_2 and the magnitude of the tunneling correction (*7*).

Experimental data for secondary isotope effects at 25°C are presented in Table 3. The agreement among multiple time points for a given experiment is high, with average errors of 1 percent for k_D/k_T and 2 percent for k_H/k_T values. Reproducibility between experiments is also excellent, with essentially identical values for all k_D/k_T measurements and a deviation of 1 percent from an average value of 1.35 ± 0.02 for k_H/k_T. Values of k_H/k_T have been calculated from the experimentally measured k_D/k_T effects with Eq. 4. These are diminished relative to the experimentally measured k_H/k_T effects, with the data in Table 3 requiring an unbelievable exponent of 10.2 ± 2.4 for agreement between measured k_D/k_T and k_H/k_T values. These results confirm Eq. 5 and indicate that quantum-mechanical effects occur in the YADH reaction.

Consequences for catalysis. In an early study (*22*), a secondary H/T isotope effect had been measured for the YADH oxidation of benzyl alcohol, yielding values identical to those in Table 3. The equilibrium isotope effect for the interconversion of alcohol to aldehyde k_H/k_T, was 1.33 ± 0.05 (*22*). The identity of kinetic and equilibrium isotope effects suggested that the transition state for alcohol oxidation was late, involving complete rehybridization at C-1 from sp^3 (alcohol-like) to sp^2 (aldehyde-like) (*30*). However, this conclusion was in direct conflict with the results of structure-reactivity correlations, which indicated an early transition state resembling the alcohol (*22*).

Our measurement of D/T secondary isotope effects (Table 3) resolves this dilemma. Note that k_D/k_T is near unity. If we assume that relatively little tunneling occurs for C–D and C–T cleavage, this ratio approaches a "pure" value, which reflects the true change in bond rehybridization at C-1 of substrate in the transition state. Application of Eq. 4 provides a secondary kinetic H/T isotope effect, k_H/k_T = 1.11 ± 0.02, that can be compared with the equilibrium isotope effect of 1.33 ± 0.05. This comparison indicates a relatively early transition state, involving only modest changes in bond rehybridization at C-1 of substrate. Thus, through the use of an isotope effect measurement that reduces the tunneling component to the reaction coordinate, both secondary isotope effects and structure-reactivity correlations lead to a similar conclusion regarding transition-state structure. One must recognize that the inflated value seen for the secondary H/T isotope effect is not simply a consequence of coupled motion, which is also present in D/T measurements (*7, 26*). Rather, it is a consequence of protium tunneling at H_1, which, together with coupled motion, allows the propagation of quantum-mechanical effects into the motion of H_2 at the transition state (*31*).

Given the establishment of hydrogen tunneling in the YADH reaction, it becomes important to integrate this phenomenon into our understanding of enzyme catalysis. First, we note that for hydrogen tunneling to be significant in enzyme catalysis, a reaction coordinate structure is required that does not involve a large, direct coupling of protein motion to the bond cleavage event. Tight coupling of the movement of protein side chains to hydrogen transfer inflates the mass of the transferred particle and decreases the tunneling probability.

Electron tunneling between metal sites in proteins has been extensively modeled by Marcus theory (*32*). In this theory, the electron motion is fully quantum mechanical, with the observed temperature dependencies arising from ligand reorganizations re-

quired for effective electron transfer. An analogous interpretation of nuclear tunneling in the YADH reaction would involve a model in which thermally activated protein motion is required for H, D, and T transfer. This motion allows the achievement of an optimal distance between donor and acceptor atom, followed by a quantum-mechanical penetration of the barrier by hydrogen. In such a model the temperature dependence for substrate oxidation would be nearly independent of isotopic substitution and would lead to large differences in Arrhenius prefactors for H- and D-containing substrates, that is, $A_H/A_D >> 1$ (*33*). However, semilogarithmic plots of k_H/k_T and k_D/k_T versus temperature extrapolate to a value of A_H/A_D near the semiclassical limit ($A_H/A_D = 1.1 \pm 0.1$) (Fig. 3). This result effectively rules out "classic" Marcus-type mechanisms for hydrogen transfer in the YADH reaction (*34*).

In light of the above discussion a picture begins to emerge for hydrogen transfer in YADH which involves a combination of thermally activated, over-the-barrier processes and through-the-barrier events. Although D tunneling may contribute relatively little to the rate, given the observation of semiclassical effects on prefactor terms of $A_H/A_D = 1.1 \pm 0.1$ and enthalpies of activation of $E_D - E_H = 3.3 \pm 1.3$ kJ/mol, interpretation of these effects is complicated by the presence of coupled motion as well as tunneling. Some insight into possible magnitudes for $Q_t(H)$ and $Q_t(D)$ comes from an earlier computational study of Huskey and Schowen (*26*). The magnitude of isotope effects was shown to vary greatly, depending on the extent of contributions from coupled motion and tunneling with relatively small primary isotope effects arising in reactions characterized by substantial tunneling. Through the use of the truncated Bell equation (Eq. 1), which is valid for moderate amounts of tunneling, values of $Q_t(H) = 4$ and $Q_t(D) = 2.5$ have been estimated for the reduction of ketones in the ADH reaction. Since $Q_t(L)$ reflects the ratio of rate constants for tunneling (k_{tun}) to semiclassical thermal activation (k_{sc}):

$$Q_t(L) = k_{tun}/k_{sc} \quad (10)$$

the results of Huskey and Schowen suggest a fairly sizable contribution of tunneling, ~80 and ~71 percent for net H and D transfer, respectively.

The above discussion suggests that tunneling may represent a significant pathway for catalysis at the ADH active site. Independent of the absolute magnitude of $Q_t(L)$, the detection of tunneling introduces a new probe for the quantitative characterization of enzymatic reaction barriers. We are currently modeling the temperature and mass dependencies in the YADH reactions, in an effort to describe the shape (both width and height) of the reaction barrier. In the course of these computations, we have begun to consider a possible role for protein motion in the bond-cleavage event. Examination of existing structures for ternary complexes in the horse liver ADH reaction (*35, 36*) and in dihydrofolate reductase (*37*) indicates bond distances of 3.4 to 3.6 Å between C-1 of the substrate and C-4 of the cofactor. Although these distances may contain considerable error [especially when model-building is necessary to obtain a catalytically relevant structure (*36*)], they are too long for either a semiclassical hydrogen transfer or a reaction involving tunneling of hydrogen through the barrier (*38*). It appears that the available (static) x-ray structures do not provide a realistic barrier width and that changes in active-site geometry are required before reaction can occur. These changes need not involve a discrete protein conformational change, since protein breathing motions alone may provide the reduction in barrier width required for a subsequent hydrogen-transfer event to occur.

REFERENCES AND NOTES

1. D. De Vault, *Quantum Mechanical Tunneling in Biological Systems* (Cambridge Univ. Press, Cambridge, ed. 2, 1984).
2. A. W. Axup, M. Albin, S. L. Mayo, R. J. Crutchley, H. B. Gray, *J. Am. Chem. Soc.* **110**, 435 (1988), and references therein.
3. R. P. Bell, *The Tunnel Effect in Chemistry* (Chapman & Hall, New York, 1980).
4. We use hydrogen and L to refer to all isotopes, protium or H to refer to ^{1}H, deuterium or D to refer to ^{2}H, and tritium or T to refer to ^{3}H.
5. J. R. Knowles and W. J. Albery, *Acc. Chem. Res.* **10**, 105 (1975).
6. W. W. Cleland, *ibid.* **8**, 145 (1975).
7. W. H. Saunders, Jr., *J. Am. Chem. Soc.* **107**, 164 (1985).
8. Although m in Eq. 2 refers to reduced mass, this is approximated by the mass of H (or D and T) for hydrogen transfer between heavy atoms.
9. Since a reaction coordinate involves bond cleavage, F is negative and $\nu\ddagger$ is imaginary.
10. K. P. Nambiar, D. M. Stauffer, P. A. Kolodziej, S. A. Benner, *J. Am. Chem. Soc.* **105**, 5886 (1983).
11. J. R. De La Vega, *Acc. Chem. Res.* **15**, 185 (1982).
12. J. W. Verhoeven, G. J. Koomen, S. M. Van Der Kerk, *Rec. Trav. Chim. Pays-Bas.* **105**, 343 (1986).
13. E. F. Caldin, S. Mateo, *J. Chem. Soc. Faraday Trans. I* **71**, 1876 (1975); N. Sugimoto, M. Sasaki, J. Osugi, *Bull. Chem. Soc. Jpn.* **57**, 366 (1984), and references therein.
14. P. A. Bartlett and C. K. Marlowe, *Biochemistry* **26**, 8553 (1987).
15. L. Pauling, *Am. Sci.* **36**, 51 (1948).
16. J. Rodgers, D. A. Femec, R. L. Schowen, *J. Am. Chem. Soc.* **104**, 3263 (1982).
17. C. G. Swain, E. C. Stivers, J. F. Reuwer, Jr., L. J. Schaad, *ibid.* **80**, 5885 (1958).
18. A. Streitwieser, Jr., *et al.*, *ibid.* **93**, 5096 (1971); A. Streitwieser, Jr., *et al.*, *ibid.* **95**, 4254 (1973).
19. D. B. Northrop, in *Isotope Effects on Enzyme-Catalyzed Reactions*, W. W. Cleland *et al.*, Eds. (University Park Press, Baltimore, MD, 1977), pp. 122–152.
20. W. J. Albery and J. R. Knowles, *J. Am. Chem. Soc.* **99**, 637 (1977).
21. As pointed out by D. B. Northrop (personal communication), H/T and D/T isotope effects can be formulated in reciprocal forms as T/H and T/D, respectively. In this instance, a common commitment, C_T, relates observed and intrinsic isotope effects. However, the impact of the commitment on the expression of the isotope effect is the same as revealed by Eqs. 6 and 7, reflecting the relative contributions of k_T/k_H versus C_T and k_T/k_D versus C_T to observed isotope effects. Since $k_T/k_D > k_T/k_H$, the expression of $(V/K_m)_T/(V/K_m)_D$ will be less influenced by C_T than $(V/K)_T/(V/K)_H$.
22. J. P. Klinman, *Biochemistry* **15**, 2018 (1976).
23. K. M. Welsh, D. J. Creighton, J. P. Klinman, *ibid.* **19**, 2005 (1980).
24. P. F. Cook, N. J. Oppenheimer, W. W. Cleland, *ibid.* **20**, 1817 (1981).
25. L. C. Kurz and C. Frieden, *J. Am. Chem. Soc.* **102**, 4198 (1980).
26. W. P. Huskey and R. L. Schowen, *ibid.* **105**, 5704 (1983).
27. The study of D/T isotope effects requires special considerations. In the case of deuterated, tritiated benzyl alcohols, synthesis was undertaken in a stepwise fashion to allow the incorporation of deuterium prior to tritium. In this manner, aldehyde was first exchanged with deuterium from D_2O to a level of >99.8 percent D [A. W. Burgstahler, D. E. Walker, Jr., J. P. Kuebvice, R. L. Schowen, *J. Org. Chem.* **37**, 1272 (1972)]. Subsequent reduction of aldehyde to alcohol used [^{3}H]$NaBH_4$ (specific activity = 68.3 Ci/mmol). At this level of radioactivity, ~50 percent of the $NaBH_4$ contained tritium. Thus half of the alcohol produced was the desired product (containing D and T at C-1), with the remaining ~50 percent being a contaminant (containing D and H). However, our experimental technique is unaltered by the presence of the D,H product, since all measurements involve the comparison of tritium to ^{14}C in product. The key to the successful measurement of D,T ratios is the maintenance of high levels of deuterium in tritium and ^{14}C-containing substrates. At >99.8 percent D in tritiated benzyl alcohol, no correction for the presence of H,T sample was necessary. The situation with ^{14}C-labeled substrate was somewhat different, since synthesis by $LiAlD_4$ reduction of benzoic acid led to deuterium at a level of only 98.7 percent. We have, therefore, corrected for the reaction of ^{14}C-labeled alcohol containing 0.65 percent H in the (*R*)- and (*S*)-positions.
28. Isotope effects were calculated from experimental ^{3}H/^{14}C ratios and fractional conversions f as shown below [L. C. Melander and W. H. Saunders, Jr., *Reaction Rates of Isotope Molecules* (Wiley, New York, 1980)].

$$({}^3H/{}^{14}C)_f^{k_L/k_T} = \frac{\ln(1-f)}{\ln\{1 - f[\frac{({}^3H/{}^{14}C)_f}{({}^3H/{}^{14}C)_\infty}]\}} \quad (L = H, D)$$

where $({}^3H/{}^{14}C)_f$ and $({}^3H/{}^{14}C)_\infty$ are the observed ^{3}H to ^{14}C ratios at fractional and complete conversion, respectively. In our samples, $({}^3H/{}^{14}C)_\infty$ is routinely equal to one half of $({}^3H/{}^{14}C)$ in starting material. To correct for H contamination in ^{14}C-labeled deuterated benzyl alcohol (K. Grant and J. P. Klinman, unpublished results), we first express product arising from dideuterated alcohol (98.7 percent) and alcohol that contained 0.65 percent hydrogen in the (*R*)- and (*S*)-positions as

$$P_{obs} = 0.987S_0(1 - e^{-At}) + 0.0065S_0(1 - e^{-Bt}) + 0.0065S_0(1 - e^{-Ct})$$

where A represents C–D bond cleavage and is assigned a value of unity, B is the primary H/D isotope effect (3.9 at 25°C), and C is the secondary H/D isotope effect (1.2 at 25°C). The fractional conversion for pure dideuterated material is

$$f_D = \frac{0.987S_0(1 - e^{-At})}{0.987S_0} = 1 - e^{-At}$$

and the correction r_t at time t is

$$r_t = f_{obs}/0.987\, f_D$$

where $f_{obs} = P_{obs}/S_0$. The corresponding correction for r_t at t_∞ is

$$r_\infty = f_{obs}/0.987\, f_D = 1/0.987$$

The final expression for the D/T isotope effect is

$$k_D/k_T = \frac{\ln(1 - f_D)}{\ln\{1 - f_D[\frac{(^3H/^{14}C)_f\, r_t}{(^3H/^{14}C)_\infty r_\infty}]\}} = \frac{\ln(1 - f_D)}{\ln\{1 - f_{obs}[\frac{(^3H/^{14}C)f}{(^3H/^{14}C)_\infty}]\}}$$

29. If hydrogen-isotope effects result only from differences in zero-point energy, then the following equation can be derived

$$\frac{\ln(k_D/k_T)}{\ln(k_H/k_T)} = \frac{1/(m_D)^{1/2} - 1/(m_T)^{1/2}}{1/(m_H)^{1/2} - 1/(m_T)^{1/2}}$$

The factor on the right-hand side is 3.26 for $m_H{:}m_D{:}m_T$ in the ratio of 1:2:3, or 3.34 if they are in the ratio of the reduced masses of ^{12}C–H:^{12}C–D:^{12}C–T. See (7).

30. J. L. Hogg, in *Transition States of Biochemical Processes*, R, D. Gandour and R. L. Schowen, Eds. (Plenum, New York, 1978), pp. 201–224.
31. Cleland and co-workers have reported that secondary H/D isotope effects with formate dehydrogenase were reduced from 1.23 ± 0.03 to 1.07 ± 0.02 when substrate oxidation involved C–D as opposed to C–H bond cleavage. This result was attributed to a combination of coupled motion and tunneling. See J. D. Hermes and W. W. Cleland, *J. Am. Chem. Soc.* **106**, 7263 (1984), and J. D. Hermes, S. W. Morrical, M. H. O'Leary, W. W. Cleland, *Biochemistry* **23**, 5479 (1984).
32. R. A. Marcus, *J. Phys. Chem.* **72**, 891 (1968).
33. As discussed by M. J. Stern and R. E. Weston, Jr. [*J. Chem. Phys.* **60**, 2808 (1973)], A_H/A_D is expected to be quite temperature-dependent for reactions that include a tunneling correction, leading to extrapolated values that are either significantly reduced or greater than unity. In the low-temperature limit such that tunneling dominates the reaction-coordinate motion for H, D, and T, $A_H/A_D >> 1$.
34. The relation between H/T and D/T isotope effects in the temperature range of 0° to 40°C is similar to that shown in Table 2.
35. E. Cedergren-Zeppezauer, J. P. Samama, H. Eklund, *Biochemistry* **21**, 4895 (1982).
36. H. Eklund, B. V. Plapp, J. P. Samama, C-I. Branden, *J. Biol. Chem.* **257**, 14349 (1982).
37. J. T. Bolin, D. J. Filman, D. A. Matthews, R. C. Hamlin, J. Kraut, *ibid.*, p. 13650.
38. From x-ray data, the distance between the C-4 of cofactor and the C-1 of substrate is 3.5 Å. Using the C–H bond length of 1.1 Å, and the assumption that C–H---C is linear at the transition state, the transferred hydrogen must travel 1.3 Å from reactant to product, and would travel further for a nonlinear transition state. See F. Freund, *Trends Biochem. Sci.* **6**, 142 (1981).
39. Y. Cha, C. J. Murray, J. P. Klinman, unpublished results.
40. Supported by a grant from the National Science Foundation.

16 September 1988; accepted 3 February 1989

Receptor and Antibody Epitopes in Human Growth Hormone Identified by Homolog-Scanning Mutagenesis

BRIAN C. CUNNINGHAM, PARKASH JHURANI, PETER NG, JAMES A. WELLS*

A strategy, termed homolog-scanning mutagenesis, was used to identify the epitopes on human growth hormone (hGH) for binding to its cloned liver receptor and eight different monoclonal antibodies (Mab's). Segments of sequences (7 to 30 residues long) that were derived from homologous hormones known not to bind to the hGH receptor or Mab's, were systematically substituted throughout the hGH gene to produce a set of 17 chimeric hormones. Each Mab or receptor was categorized by a particular subset of mutant hormones that disrupted binding. Each subset of the disruptive mutations mapped within close proximity on a three-dimensional model of hGH, even though the residues changed within each subset were usually distant in the primary sequence. The mapping analysis correctly predicted those Mab's which could or could not block binding of the receptor to hGH and further suggested (along with other data) that the folding of these chimeric hormones is like that of hGH. By this analysis, three discontinuous polypeptide determinants in hGH—the loop between residues 54 and 74, the central portion of helix 4 to the carboxyl terminus, and to a lesser extent the amino-terminal region of helix 1—modulate binding to the liver receptor. Homolog-scanning mutagenesis should be of general use in identifying sequences that cause functional variation among homologous proteins.

HUMAN GROWTH HORMONE (HGH) PARTICIPATES IN THE regulation of normal human growth and development. This 22-kilodalton pituitary hormone has a multitude of biological effects, including linear growth (somatogenesis), lactation, activation of macrophages, and insulin-like and diabetogenic effects (*1*). Growth hormone deficiency in children leads to dwarfism, which has been successfully treated by injection of hGH. In addition to its biological properties, the antigenicity of hGH is useful for distinguishing genetic and post-translationally modified variants of hGH (*2*), for characterizing any immunological responses to hGH when it is administered clinically, and for quantifying the hormone during circulation.

Human growth hormone is a member of a family of homologous

B. C. Cunningham and J. A. Wells are in the Department of Biomolecular Chemistry, and P. Jhurani and P. Ng are in the Department of Organic Chemistry, Genentech, Inc., 460 Point San Bruno Boulevard, South San Francisco, CA 94080.

*To whom correspondence should be addressed.